

## Variable Temperature and EPR Frequency Study of Two Aqueous Gd(III) Complexes with Unprecedented Sharp Lines

Alain Borel,<sup>\*,†,‡</sup> Hoon Kang,<sup>†</sup> Christelle Gateau,<sup>§</sup> Marinella Mazzanti,<sup>§</sup> R. B. Clarkson,<sup>||</sup> and R. Linn Belford<sup>†</sup>

*Illinois EPR Research Center and Department of Chemistry and Department of Veterinary Clinical Medicine, University of Illinois, Urbana, Illinois 61801, Institut des sciences et ingénierie chimiques, Ecole Polytechnique Fédérale de Lausanne, CH-1015 Lausanne, Switzerland, and Laboratoire de Reconnaissance Ionique and Chimie de Coordination, Service de Chimie Inorganique et Biologique (UMR-E 3 CEA-UJF), Département de Recherche Fondamentale sur la Matière Condensée, CEA-Grenoble, 38054 Grenoble, Cedex 09, France*

Received: August 23, 2006

We present an EPR study of two Gd(III) complexes in aqueous solution at multiple temperatures and EPR frequencies. These two complexes, [Gd(TPATCN)] and [Gd(DOTAM)(H<sub>2</sub>O)]<sup>3+</sup>, display remarkably sharp lines (i.e. slow transverse electron spin relaxation) in comparison with all complexes studied in the past, especially at X-band (~9.08 GHz). These unprecedented spectra even show, for the first time in solution, a distinct influence of hyperfine coupling to two magnetically active Gd isotopes (<sup>155</sup>Gd 14.8%,  $I = 3/2$ ,  $\gamma = -0.8273 \times 10^7 \text{ s}^{-1} \text{ T}^{-1}$  and <sup>157</sup>Gd, 15.65%,  $I = 3/2$ ,  $-1.0792 \times 10^7 \text{ s}^{-1} \text{ T}^{-1}$ ). The hyperfine coupling splitting in [Gd(TPATCN)] was determined accurately for a <sup>157</sup>Gd-enriched complex, and the value  $A(^{157}\text{Gd})/g\mu_B = 5.67 \text{ G}$  seems to be a good estimation for most chelates of interest. Consequently, we can safely assert that neglecting the Gd isotopes in line shape studies is not a significant source of error as long as the apparent peak-to-peak width is greater than 10–20 G. This is generally the case, except at very high EPR frequencies (>150 GHz). Analyzing the spectra within the physical model of Rast et al. we find that the slow electron spin relaxation is due to a nearly zero static ZFS. We discuss some structural features that might explain this interesting electron structure.

### Introduction

Gd(III) complexes with multidentate ligands are routinely used in medicine as contrast agents for magnetic resonance imaging (MRI). The so-called *relaxivity* quantifies the water protons magnetic relaxation rate enhancement due to the interaction with the 7 unpaired electrons of the Gd(III) center. A deeper understanding of the molecular origins of relaxivity is required in order to develop improved contrast agents. For this reason, the last two decades have witnessed many studies on the magnetic properties of these complexes, mostly using <sup>1</sup>H and <sup>17</sup>O NMR.<sup>1,2</sup> More recently, electron paramagnetic resonance (EPR) has emerged as the natural method of choice for the direct study of one important factor that influences relaxivity, namely the electron spin relaxation.<sup>3–7</sup>

Due to the toxicity of the [Gd(H<sub>2</sub>O)<sub>8</sub>]<sup>3+</sup> aqua ion, it is necessary to use chelates for potential contrast agents. The ligands are generally polyaminocarboxylates, the basic example of which is the well-known EDTA (ethylenediaminetetraacetate). However, for better stability, the denticity of the ligand must be higher than 6 for EDTA. The commercial contrast agent ligands (DOTA, DTPA, DTPA-BMA, HP-DO3A)

occupy 8 coordination sites around the metal, leaving only one available position for a water molecule. This reduced hydration number has an obviously negative impact on relaxivity, as the chemical exchange of water molecules bound to the paramagnetic center is an efficient way to enhance the overall water proton relaxation rate. It also affects the electron spin relaxation rates by changing the zero-field splitting (ZFS) due to the different ligand field. A major trend of research in recent years has been to increase the relaxivity through an increase in molecular weight<sup>8–11</sup> or binding to macromolecules<sup>12–14</sup> or an acceleration of the water exchange.<sup>15–17</sup> Although less attention has been devoted to this aspect of relaxivity, it is worthwhile to investigate alternative ligand designs that could optimize the electron spin relaxation properties.

The typical X-band EPR (9–9.5 GHz) spectrum of a Gd(III) chelate in solution is a broad, roughly Lorentzian line. The peak-to-peak width is usually between 50 and 1000 G, depending on the molecule and the temperature. At higher EPR frequencies, the lines become sharper. In this paper, we report variable temperature X- and W-band measurements on two complexes with unusually sharp lines (less than 40 G at X-band). Fairly high low-field relaxivities have been observed for the complexes of tripodal ligands<sup>18,19</sup> such as the heptadentate TPAA ( $\alpha, \alpha', \alpha''$ -nitrilotri(6-methyl-2-pyridinecarboxylate) and the nonadentate H<sub>3</sub>TPATCN<sup>20</sup> (1,4,7-tris[(6-carboxypyridin-2-yl)methyl]-1,4,7-triazacyclononane). Since the [Gd(TPATCN)] complex has no water molecule directly bound to the metal ion, it was suggested<sup>20</sup> an especially slow electron spin relaxation might be the origin of this high relaxivity (only 15% lower than [Gd-(DTPA-BMA)(H<sub>2</sub>O)] at room temperature). Another interesting

\* Corresponding author fax: +41 21 693 9805; e-mail: alain.borel@epfl.ch. Corresponding author address: Institut des sciences et ingénierie chimiques, EPFL-SB-SCGC-BCH, CH-1015 Lausanne, Switzerland.

<sup>†</sup> Illinois EPR Research Center and Department of Chemistry, University of Illinois.

<sup>‡</sup> Ecole Polytechnique Fédérale de Lausanne.

<sup>§</sup> CEA-Grenoble.

<sup>||</sup> Illinois EPR Research Center and Department of Veterinary Clinical Medicine, University of Illinois.

compound is the macrocyclic complex  $[\text{Gd}(\text{DOTAM})(\text{H}_2\text{O})]^{3+}$  (DOTAM = 1,4,7,10-tetraazacyclododecane-1,4,7,10-tetraacetamide), a DOTA derivative. Although useless as a contrast agent, it has been the subject of a number of studies, yielding for example precious information about the possible correlations between internal motions of the ligand and water exchange.<sup>21</sup> We examine the effect of concentration on the line width and take into account the presence of two minor isotopes with nonzero nuclear spin ( $^{155}\text{Gd}$  and  $^{157}\text{Gd}$ , 14.8 and 15.65% natural abundance,  $\gamma = -0.8273 \times 10^7$  and  $-1.0792 \times 10^7 \text{ s}^{-1} \text{ T}^{-1}$ , both  $I = 3/2$ ). The high-frequency, high-temperature spectra show a non-negligible effect of these isotopes on the line shape. To clarify this point, we also prepared a  $^{157}\text{Gd}$ -enriched complex and unambiguously measured the hyperfine coupling constant. We compare this coupling constant with the published value for the Eu(II) aqua ion in order to generalize this result for all Gd(III) complexes of interest.

### Experimental Section

**[Gd(TPATCN)].** The synthesis of [Gd(TPATCN)] has been presented elsewhere.<sup>20</sup> A 13.45 mM sample was prepared. Successive dilutions with distilled water yielded samples with 5.1, 1.8, and 0.60 mM, respectively. Enriched  $^{157}\text{Gd}$  oxide (93.62%  $^{157}\text{Gd}$ , 0.615%  $^{155}\text{Gd}$ ) was purchased from the Oak Ridge National Laboratory (Oak Ridge, TN, U.S.A.), and the complex was prepared in solution (0.39 mM) using the published procedure after dissolution of the oxide in HCL 36.5%.

**[Gd(DOTAM)(H<sub>2</sub>O)]<sup>3+</sup>.** Cyclen (0.500 g, 2.91 mmol), bromoacetamide (1.810 g, 13.12 mmol), and triethylamine (2 mL, 14.38 mmol) were heated at reflux in anhydrous ethanol for 4 h. The DOTAM ligand precipitated out during the course of the reaction and was recrystallized from boiling ethanol/water; yield 61%.  $\text{Gd}(\text{SO}_3\text{CF}_3)_3$  (0.63 mmol) in 75 mL of anhydrous ethanol was treated with DOTAM (0.250 g, 0.63 mmol) in 225 mL of ethanol. The mixture was heated at reflux under nitrogen for 3.5 h following the dissolution of DOTAM. The solution was concentrated in vacuo, and hexane was added until cloudiness was observed. Yields were greater than 55%. Satisfactory microanalytical data were obtained for all compounds. <sup>1</sup>H NMR ( $\text{CD}_3\text{CN}$ ): [La(DOTAM)]-( $\text{CF}_3\text{SO}_3$ )<sub>3</sub> (−10 °C):  $\delta = 2.42$  (NCH<sub>2</sub> (equatorial), d,  $J(\text{C,H}) = 14.8$  Hz), 2.56 (NCH<sub>2</sub> (equatorial), d,  $J(\text{C,H}) = 13.6$  Hz), 2.85 (NCH<sub>2</sub> (axial), pseudo t), 3.35 (NCH<sub>2</sub> and CH<sub>2</sub>C(O)NH<sub>2</sub>, m), 3.84 (CH<sub>2</sub>C(O)NH<sub>2</sub>, d,  $J(\text{C,H}) = 16.4$  Hz), 7.27 (NH<sub>2</sub>, s), 7.81 (NH<sub>2</sub>,s). <sup>13</sup>C NMR ( $\text{CD}_3\text{CN}$ ): [La(DOTAM)]-( $\text{CF}_3\text{SO}_3$ )<sub>3</sub> (−20 °C):  $\delta = 50.1, 54.3$  (NCH<sub>2</sub>, ring), 58.9 (NCH<sub>2</sub>, amide), 178.8 (C(O)NH<sub>2</sub>). A 10 mM solution was prepared and diluted to 4, 1, and 0.24 mM.

**EPR Spectroscopy and Analysis.** Continuous-wave EPR spectra were recorded at X- (~9.08 GHz) and W-band (~94.2 GHz) at temperatures between 0 and 70 Celsius. The X-band spectrometer was a Varian E-112 instrument, and the magnetic field calibration was performed using a Varian E-500 gaussmeter. The W-band spectrometer is a custom-built instrument, and the signal of Mn(II) in a plasticine sample<sup>22</sup> was used as a reference for the field calibration. The frequency was measured by a digital divider/counter. The temperature was adjusted using standard VT controllers and accurately measured with a copper–constantan thermocouple.

The spectra were subsequently analyzed using the program NMRICMA.<sup>23</sup> The peak-to-peak widths  $\Delta H_{\text{pp}}$ , central fields  $B_0$ , and hyperfine coupling constants were extracted by fitting a superposition of Lorentzians to the experimental spectra, with automatic phase and baseline adjustment. We then analyzed the

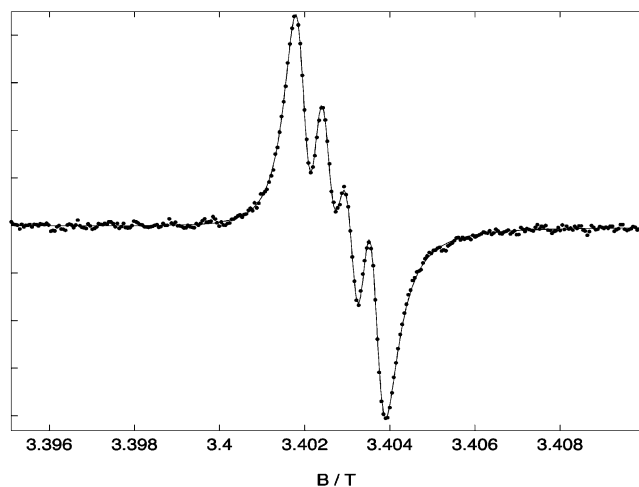


**Figure 1.** W-band EPR spectrum of  $[\text{}^{157}\text{Gd}(\text{TPATCN})]$  (93.62% enrichment) at  $T = 342.5$  K. Dots: experimental spectrum. Solid line: best multi-Lorentzian fit.

line widths and shifts within the framework of the Rast model,<sup>7,24,25</sup> using only the reduced values  $\Delta H_{\text{pp}}$  and  $B_0$  instead of the full line shape. This model assumes that the electron spin relaxation is determined by the so-called static or average ZFS, which is rapidly modulated by molecular tumbling, and by the transient ZFS, which is modulated by random distortions of the complex. Here we limited the static and transient ZFS to second order, although fourth- and sixth-order terms are also possible for a spin  $S = 7/2$ . The least-squares fit procedure yields the following parameters: the static ZFS magnitude parameter  $a_2$ , the rotational correlation time  $\tau_{\text{R}}$  and activation energy  $E_{\text{R}}$ , the transient ZFS magnitude  $a_{2\text{T}}$ , the associated correlation time  $\tau_{\text{v}}$  and activation energy  $E_{\text{v}}$ , plus the natural  $g$ -factor.

### Results and Discussion

**Hyperfine Effects.** The EPR spectra we observed for the 13.45 mM [Gd(TPATCN)] solution showed noticeable divergence from a simple Lorentzian derivative, especially at W-band and high temperature. The apparent peak-to-peak width was in the 10–20 G region at X-band and 8–12 G at W-band. The sharpest spectra showed divergences from the ideal derivative Lorentzian line shape, suggesting a possible inhomogeneous broadening. To solve this question unambiguously, we prepared and observed at W-band a 93.62%  $^{157}\text{Gd}$ -enriched complex. Figure 1 clearly shows the well-resolved coupling with the  $I = 3/2$   $^{157}\text{Gd}$  nucleus, with a coupling constant  $A/g\mu_{\text{B}} = 5.67$  G. The corresponding coupling constant for the  $^{155}\text{Gd}$  isotope, due to the gyromagnetic ratio, is 4.34 G. We can compare this value with that measured for the Eu(II) aqua ion. Europium has two stable  $I = 5/2$  isotopes,  $^{151}\text{Eu}$  (47.8%,  $\gamma = 6.5477 \times 10^7 \text{ s}^{-1} \text{ T}^{-1}$ ) and  $^{153}\text{Eu}$  (52.2%,  $\gamma = 2.9371 \times 10^7 \text{ s}^{-1} \text{ T}^{-1}$ ). The reported value for  $[\text{}^{151}\text{Eu}(\text{H}_2\text{O})_8]^{2+}$  is  $A/g\mu_{\text{B}} = 37.3$  G.<sup>26</sup> Since the coupling constant is proportional to the electron spin density at the nucleus and to the nuclear gyromagnetic ratio, we can calculate an equivalent  $^{157}\text{Gd}^{3+}$  value of 6.15 G, fairly close to our observed value. Examples of Gd(III) doped into various solid matrices can be found in the literature, such as  $A(^{157}\text{Gd})/g\mu_{\text{B}} = 5.34$  G in  $\text{Bi}_2\text{Mg}_3(\text{NO}_3)_{12}$ , 5.7 G in  $\text{LaCl}_3$ ,<sup>27</sup> 15.0241 MHz  $\approx 5.37$  G in  $\text{SrCl}_2$ ,<sup>28</sup> 5.702 G in  $\text{CaCO}_3$ ,<sup>29</sup> 6.55 G in  $\text{La}(\text{CH}_3\text{CH}_2\text{SO}_4)_3$ ,<sup>30</sup> 14.9 and 13.4 MHz  $\approx 5.33$ , and 4.79 G for two different sites with some hyperfine anisotropy in  $\text{Y}_2\text{O}_3$ .<sup>31</sup> All values are in fair or very good agreement with our observation, considering the variety of host lattices. This is not surprising since we expect the half-filled 4f shell to be left

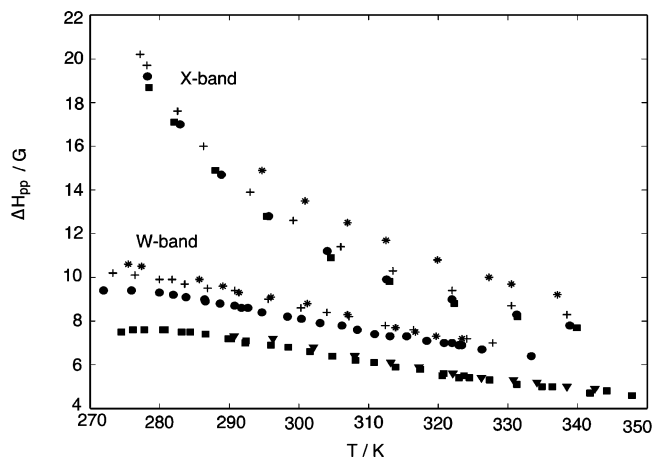


**Figure 2.** Experimental peak-to-peak widths of [Gd(TPATCN)] at X- and W-band: (\*) 13.45 mM, (+) 5.1 mM, (●) 1.8 mM, (■) 0.60 mM, (▼) 0.39 mM.

relatively undisturbed by any kind of ligand field, so the spin density at the nucleus will be essentially the same for most complexes.

Considering these results, we can safely assume a coupling constant  $A(^{157}\text{Gd})/g\mu_B = 5.5\text{--}6\text{ G}$  for all polyaminocarboxylates or even for most molecular complexes. The error induced by a neglect of the two NMR-active isotopes is completely negligible for peak-to-peak widths larger than 50 G. Between 50 and 10 G, the overall line shape is still Lorentzian, but the actual width is 1 G less than the apparent peak-to-peak width. Below 10 G, the difference between the actual and the apparent peak-to-peak width is about 1.5 G, and at 5 G the line shape diverges from the ideal Lorentzian, especially in the wings. The outer  $m_I = -3/2$  and  $+3/2$  transitions should be observable in natural abundance as partly resolved  $^{155}/^{157}\text{Gd}$  satellites for peak-to-peak widths lower than 3 G. Since most Gd(III) complexes studied to date have lines wider than 100 G at X-band, we can expect the  $^{155}/^{157}\text{Gd}$  hyperfine to be an important factor for the line shape analysis only at EPR frequencies above 100 GHz.

**Relaxation Effects.** The subsequent analysis (extraction of peak-to-peak widths and central fields) was performed by fixing the hyperfine coupling constants and adjusting to the experimental spectrum a superposition of 4 ( $^{155}\text{Gd}$ ) + 4 ( $^{157}\text{Gd}$ ) + 1 (other isotopes) Lorentzians, taking into account the natural isotopic abundances. Figure 2 shows the resulting peak-to-peak widths. No effect of the concentration on the central fields was observed.

The Gd(III) concentration has a measurable effect on the peak-to-peak widths even at X-band. At X-band, this effect

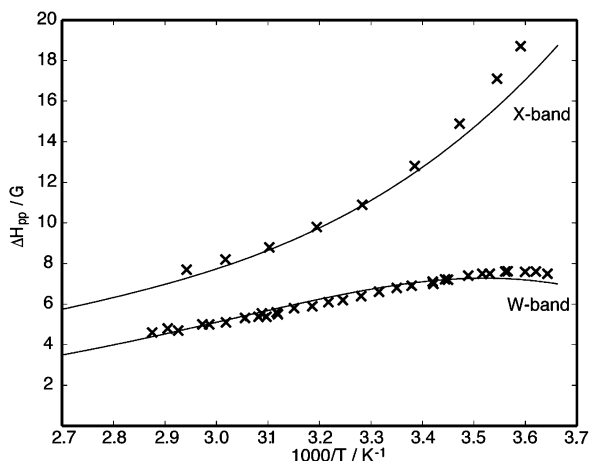


**TABLE 1: Electron Spin Relaxation Parameters from Fit**

complex	[Gd(TPATCN)]	[Gd(DOTAM)(H <sub>2</sub> O)] <sup>3+</sup>
$a_2/10^{10}\text{ s}^{-1}$	0.0661	0.0273
$\tau_R = 1/D_R/\text{ps}$	500	500
$E_R/\text{kJ mol}^{-1}$	17	17
$a_{2T}/10^{-10}\text{ s}^{-1}$	0.2322	0.3412
$\tau_V/\text{ps}$	1.19	2.03
$E_V/\text{kJ mol}^{-1}$	11.6	11.3
$g$	1.9915	1.9913

vanishes at 1.8 mM and below, whereas the “infinite dilution limit” is only reached at 0.60 mM at W-band. Therefore, we systematically used the 0.60 mM and below for our fitting of the electron spin relaxation parameters. The actual value of the rotational correlation time is not known for this complex, but we can assume it is close to that of [Gd(DOTA)(H<sub>2</sub>O)]<sup>-</sup> of similar size. We used a fixed value of 500 ps for  $\tau_R$  and 17 kJ/mol for  $E_R$  in the fitting procedure. The experimental points and theoretical curves are represented in Figure 3, and the resulting parameters can be found in Table 1.

[Gd(DOTAM)(H<sub>2</sub>O)]<sup>3+</sup> displays slightly broader lines, especially at X-band. We extracted the peak-to-peak widths and central fields from the experimental spectrum assuming the same hyperfine coupling constant as for [Gd(TPATCN)]. Indeed, the high-temperature W-band spectra yielded a value of 5.5–6.0 G for  $A(^{157}\text{Gd})/g\mu_B$  when a free adjustment was allowed. The measured line widths can be seen in Figure 4. The concentration effect is only apparent at W-band. The signal-to-noise ratio for the 0.24 mM concentration was not as good as for the 1 mM solution at W-band and low temperature, so we used the latter for the peak-to-peak width and central fields analysis. As for [Gd(TPATCN)], we used a fixed value of 500 ps for  $\tau_R$  and 17 kJ/mol for  $E_R$ . The experimental points and theoretical curves are represented in Figure 5, and the resulting parameters are reported in Table 1.

The agreement between the experimental and simulated values is very good. The peak-to-peak widths are very well reproduced in both cases. For [Gd(TPATCN)], the error in the central field value is less than 0.2 G at X-band and 0.1–0.4 G at W-band. For [Gd(DOTAM)(H<sub>2</sub>O)]<sup>3+</sup>, it is slightly larger (0.1–0.4 G at X-band, 0.7–1.0 G at W-band).

The parameters extracted from the peak-to-peak widths and apparent  $g$ -factors (Table 1) are generally similar to those obtained for other complexes in solution, with the exception of the static ZFS magnitude parameter. For both complexes,  $a_2$  is about 1 order of magnitude smaller than for the other reported complexes. This indeed appears to be the origin of their extraordinarily sharp X-band EPR lines. In general, the static

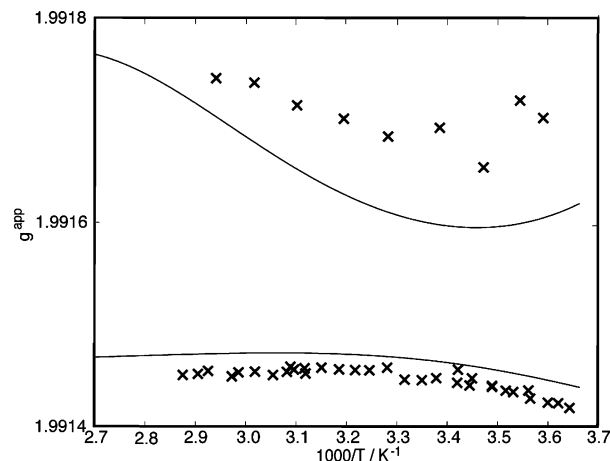


**Figure 3.** Peak-to-peak widths and apparent  $g$ -factors for [Gd(TPATCN)]: experimental points and fitted curves.

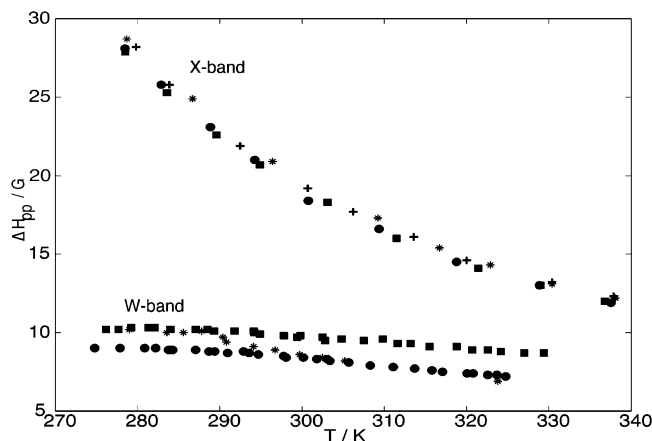


**Figure 4.** Peak-to-peak widths of  $[\text{Gd}(\text{DOTAM})(\text{H}_2\text{O})]^{3+}$  at X- and W-band: (■) 10 mM, (+) 4 mM, (●) 1 mM, (\*) 0.24 mM.

ZFS is expected to play a dominant role in the electron spin relaxation at the lower frequencies owing to the longer correlation time (rotation, 10–1000 ps, compared to vibrations  $\sim 1$  ps). As frequency increases (Q-band and above), the static ZFS spectral densities decay and the transient ZFS becomes the dominant contribution. For  $[\text{Gd}(\text{TPATCN})]$  and  $[\text{Gd}(\text{DOTAM})(\text{H}_2\text{O})]^{3+}$ , the static ZFS is so small that the transient ZFS modulation provides the dominant relaxation mechanism at all frequencies. We note that this makes them the first Gd(III) chelates where the old model of pseudorotational transient ZFS modulation proposed by Hudson and Lewis<sup>32</sup> might actually be justified.

Of course, the question of the origin of this almost negligible static ZFS is of the utmost importance. Unfortunately, the relationship between the chelate structure and the zero field splitting is still far from clear. At this point, we can only offer qualitative arguments and hypotheses. First of all, the two complexes presented in this paper have in common a rather symmetrical structure (point group  $C_4$  for  $[\text{Gd}(\text{DOTAM})(\text{H}_2\text{O})]^{3+}$  and  $C_3$  for  $[\text{Gd}(\text{TPATCN})]$ ). From group theoretical considerations, one can see that this is not enough to rule out a static ZFS. The  $S = 7/2$  manifold will always be split by a second-order ZFS for symmetries lower than  $O_h$ . However, the axial symmetry at least removes rhombic terms from the spin Hamiltonian. The scarce experimental EPR data available for gadolinium complexes in solution do not allow broad generalizations, but one can observe that the complexes based on the so-called acyclic ligands (such as  $[\text{Gd}(\text{DTPA})(\text{H}_2\text{O})]^{2-}$  and  $[\text{Gd}(\text{DTPA-BMA})(\text{H}_2\text{O})]$ ) appear to have a larger static ZFS

(DTPA:  $a_2 = 0.92 \times 10^{10} \text{ s}^{-1}$ ,  $a_{2T} = 0.43 \times 10^{10} \text{ s}^{-1}$ ; DTPA-BMA:  $a_2 = 0.82 \times 10^{10} \text{ s}^{-1}$ ,  $a_{2T} = 0.44 \times 10^{10} \text{ s}^{-1}$ ),<sup>25</sup> and thus a faster electron spin relaxation at X-band, leading to broader EPR lines compared with the macrocyclic DOTA-like complexes (DOTA:  $a_2 = 0.35 \times 10^{10} \text{ s}^{-1}$ ,  $a_{2T} = 0.43 \times 10^{10} \text{ s}^{-1}$ ).<sup>7,33</sup> The lower symmetry of the Gd(III) coordination polyhedron in the acyclic compounds induces a rhombic ZFS (i.e.  $E \neq 0$ ), with a significant impact on the overall ZFS magnitude parameters  $a_2 = [(B_2)^2 + (B_2')^2]^{1/2} = [2/3D^2 + 2E^2]^{1/2} = \Delta$ .

Another factor that might decrease the ZFS is the nature of the atoms bound to the metal. Six out of nine coordination sites in  $[\text{Gd}(\text{TPATCN})]$  are occupied by nitrogen atoms instead of oxygen atoms. The less electronegative nitrogen will produce a weaker ligand field than an oxygen atom in a carboxylate or hydroxide group. Since the ligand field has an indubitable influence on the ZFS, one may assume that the nitrogen vs oxygen ratio in the coordination polyhedron is a possible way toward tuning the static ZFS. Incidentally, we can rule out the pyridine ligands as the exclusive cause for the weak zero field splitting. The  $[\text{Gd}(\text{TPAA})(\text{H}_2\text{O})_2]$  analogue also contains three pyridine groups but only a tertiary amine instead of the triazacyclononane moiety. Relaxivity<sup>18,19</sup> and preliminary W-band EPR measurements ( $\Delta H_{\text{pp}} = 20\text{--}35$  G depending on the temperature, broader than  $[\text{Gd}(\text{DTPA})(\text{H}_2\text{O})]^{2-}$  in similar conditions) indicate that its electron spin relaxation is not slower than what has been observed for the common polyaminocarboxylate complexes. Symmetry must be considered as well. On the NMR time scale,  $[\text{Gd}(\text{TPAA})(\text{H}_2\text{O})_2]$  belongs to the  $C_{3v}$  point group. This would in principle be favorable for a slow electron spin relaxation, but the structure is clearly averaged over time as the inner sphere water molecules break the coordination polyhedron symmetry. However, the water exchange rate has not been determined due to a low solubility, and thus it is not possible to say whether the complex also has a  $C_{3v}$  symmetry on the EPR time scale. The case of  $[\text{Gd}(\text{DOTAM})(\text{H}_2\text{O})]^{3+}$  is slightly different, since the coordination polyhedron is essentially the same as in  $[\text{Gd}(\text{DOTA})(\text{H}_2\text{O})]^-$ . However, the substitution of the four carboxylate groups of DOTA<sup>4-</sup> by four amide groups is clearly not innocent from the electron spin point of view. Again, one may assume that an oxygen atom in the less polar amide will induce a weaker ligand field as well as decrease the obvious electric potential anisotropy in the macrocyclic complex.<sup>34</sup>

The explanations above being necessarily tentative, we feel that further theoretical studies are required on both complexes.

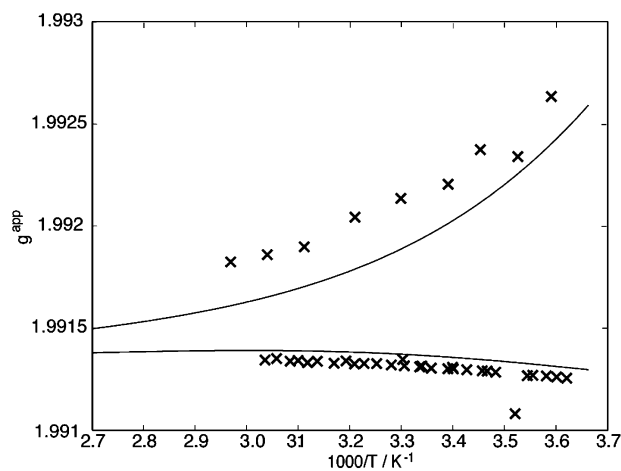
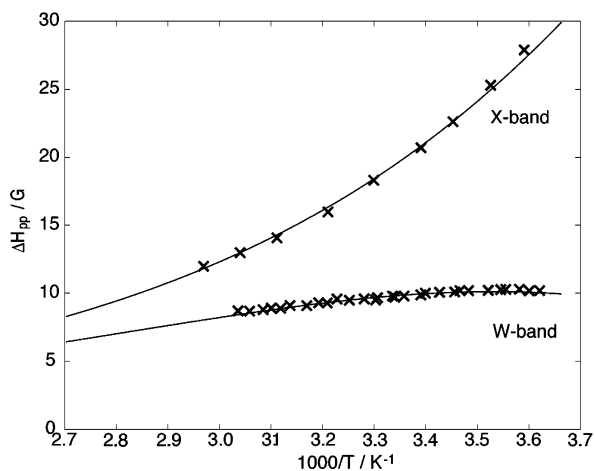


**Figure 5.** Peak-to-peak widths and apparent  $g$ -factors for  $[\text{Gd}(\text{DOTAM})(\text{H}_2\text{O})]^{3+}$ : experimental points and fitted curves.

Future quantum chemical calculations might help us elucidate the structural origins of the Gd(III) ZFS, as demonstrated by Bencini et al.<sup>35</sup> for d elements.

## Conclusion

This work presents a variable temperature study of two Gd(III) chelates, [Gd(TPATCN)] and [Gd(DOTAM)(H<sub>2</sub>O)]<sup>3+</sup>, in aqueous solution using X- and W-band continuous wave EPR. Both complexes display extraordinarily sharp lines at X-band. At W-band, the spectrum of [Gd(TPATCN)] can be analyzed only by taking into account the minor <sup>155</sup>Gd and <sup>157</sup>Gd isotopes (both with nuclear spin  $I = 3/2$ ) and their hyperfine coupling with the  $S = 7/2$  electron spin. The estimations of the coupling constant were unambiguously confirmed using a <sup>157</sup>Gd-enriched complex, yielding a final value  $A(^{157}\text{Gd})/g\mu_B = 5.67$  G. Comparison with published data on the Eu(II) aqua ion and Gd(III) in various solid matrices shows that this value should be a good estimation for most Gd(III) complexes. Indeed it also appears to hold for [Gd(DOTAM)(H<sub>2</sub>O)]<sup>3+</sup>. The knowledge of the coupling constant allows us to discuss the influence of the hyperfine structure on the line shape, which should generally be negligible except at very high EPR frequencies when the lines become increasingly sharp.

The analysis of the EPR line widths and positions using the static + transient ZFS modulation relaxation mechanism of Rast et al. indicates that the very sharp X-band lines of both complexes are consequences of a nearly zero static ZFS. No final explanation for this being available at this point, we trust that [Gd(TPATCN)] and [Gd(DOTAM)(H<sub>2</sub>O)]<sup>3+</sup> will be exciting candidates for future theoretical studies.

**Acknowledgment.** We thank the National Institute of Health (PO1 CA91597 and RO1 RR01811), the Petroleum Research Fund of the American Chemical Society, and the Swiss National Science Foundation for their financial support. We also thank Dr. Frank Dunand (Ecole Polytechnique Fédérale de Lausanne) for his help in initiating this project and Dr. Mark Nilges (University of Illinois) for his expert assistance with the EPR experiments.

**Supporting Information Available:** Complete EPR measurements (peak-to-peak widths and central fields, together with the equivalent apparent  $g$ -factor) as a function of the temperature, spectrometer frequency, and gadolinium concentration. This material is available free of charge via the Internet at <http://pubs.acs.org>.

## References and Notes

- (1) Caravan, P.; Ellison, J. J.; McMurry, T. J.; Lauffer, R. B. *Chem. Rev.* **1999**, *99*, 2293–2352.
- (2) Merbach, A. E.; Tóth, É. *The Chemistry of Contrast Agents in Medical Magnetic Resonance Imaging*; John Wiley & Sons, Ltd.: Chichester, U.K., 2001.
- (3) Powell, D. H.; Merbach, A. E.; Gonzalez, G.; Brücher, E.; Micskei, K.; Ottaviani, M. F.; Köhler, K.; von Zelewsky, A.; Grinberg, O. Y.; Lebedev, Y. S. *Helv. Chim. Acta* **1993**, *76*, 2129–2146.
- (4) Sur, S. K.; Bryant, R. G. *J. Phys. Chem.* **1995**, *99*, 6301–6308.
- (5) Clarkson, R. B.; Smirnov, A. I.; Smirnova, T. I.; Kang, H.; Belford, R. L.; Earle, K.; Freed, J. H. *Mol. Phys.* **1998**, *96*, 1325–1332.
- (6) Borel, A.; Tóth, É.; Helm, L.; Jánossy, A.; Merbach, A. E. *Phys. Chem. Chem. Phys.* **2000**, *2*, 1311–1318.
- (7) Rast, S.; Borel, A.; Helm, L.; Belorizky, E.; Fries, P. H.; Merbach, A. E. *J. Am. Chem. Soc.* **2001**, *123*, 2637–2644.
- (8) Tóth, É.; Pubanz, D.; Vauthey, S.; Helm, L.; Merbach, A. E. *Chem. Eur. J.* **1996**, *2*, 1607–1615.
- (9) Dunand, F. A.; Tóth, É.; Hollister, R.; Merbach, A. E. *J. Biol. Inorg. Chem.* **2001**, *6*, 247–255.
- (10) Nicolle, G. M.; Tóth, É.; Eisenwiener, K. P.; Macke, H. R.; Merbach, A. E. *J. Biol. Inorg. Chem.* **2002**, *7*, 757–769.
- (11) Nicolle, G. M.; Tóth, É.; Schmitt-Willich, H.; Raduchel, B.; Merbach, A. E. *Chem.–Eur. J.* **2002**, *8*, 1040–1048.
- (12) Aime, S.; Botta, M.; Fasano, M.; Crich, G. S.; Terreno, E. *J. Biol. Inorg. Chem.* **1996**, *1*, 312–319.
- (13) Caravan, P.; Greenfield, M. T.; Li, X. D.; Sherry, A. D. *Inorg. Chem.* **2001**, *40*, 6580–6587.
- (14) Caravan, P.; Cloutier, N. J.; Greenfield, M. T.; McDermid, S. A.; Dunham, S. U.; Bulte, J. W. M.; Amedio, J. C.; Looby, R. J.; Supkowski, R. M.; Horrocks, W. D.; McMurry, T. J.; Lauffer, R. B. *J. Am. Chem. Soc.* **2002**, *124*, 3152–3162.
- (15) Tóth, É.; Pubanz, D.; Vauthey, S.; Helm, L.; Merbach, A. E. *Chem. Eur. J.* **1996**, *2*, 209–217.
- (16) Tóth, É.; Burai, L.; Brucher, E.; Merbach, A. E. *J. Chem. Soc., Dalton Trans.* **1997**, 1587–1594.
- (17) Aime, S.; Barge, A.; Borel, A.; Botta, M.; Chemerisov, S.; Merbach, A. E.; Müller, U.; Pubanz, D. *Inorg. Chem.* **1997**, *36*, 5104–5112.
- (18) Bretonniere, Y.; Mazzanti, M.; Pecauc, J.; Dunand, F. A.; Merbach, A. E. *Inorg. Chem.* **2001**, *40*, 6737–6745.
- (19) Bretonniere, Y.; Mazzanti, M.; Pecauc, J.; Dunand, F. A.; Merbach, A. E. *Chem. Commun.* **2001**, 621–622.
- (20) Gateau, C.; Mazzanti, M.; Pecauc, J.; Dunand, F. A.; Merbach, A. E. *J. Chem. Soc. Dalton Trans.* **2003**, *12*, 2428–2433.
- (21) Dunand, F. A.; Aime, S.; Merbach, A. E. *J. Am. Chem. Soc.* **2000**, *122*, 1506–1512.
- (22) Raghavachari, K.; Anderson, J. B. *J. Phys. Chem.* **1996**, *100*, 12960–12973.
- (23) Helm, L.; Borel, A. 2.7 ed.; ICMA: Lausanne, 2000.
- (24) Rast, S.; Fries, P. H.; Belorizky, E. *J. Chim. Phys.* **1999**, *96*, 1543–1550.
- (25) Rast, S.; Fries, P. H.; Belorizky, E. *J. Chem. Phys.* **2000**, *113*, 8724–8735.
- (26) Caravan, P.; Tóth, É.; Rockenbauer, A.; Merbach, A. E. *J. Am. Chem. Soc.* **1999**, *121*, 10403.
- (27) Low, W. *Phys. Rev.* **1956**, *103*, 1309–1309.
- (28) Vanormondt, D.; Reddy, K. V.; Vanast, M. A.; Denhartog, H. W.; Bijvank, E. *J. Magn. Reson.* **1980**, *37*, 195–204.
- (29) Marshall, S. A.; Serway, R. A. *Phys. Rev.* **1968**, *171*, 345–349.
- (30) Bernstein, E. R.; Dobbs, G. M. *Phys. Rev. B* **1975**, *11*, 4623–4638.
- (31) Marshall, S. A.; Marshall, T.; Yuster, P. H. *Phys. Rev. B* **1982**, *25*, 1505–1513.
- (32) Hudson, A.; Lewis, J. W. E. *Trans. Faraday Soc.* **1970**, *66*, 1297–1301.
- (33) Borel, A.; Helm, L.; Merbach, A. E.; Atsarksin, V. A.; Demidov, V. V.; Odintsov, B. M.; Belford, R. L.; Clarkson, R. B. *J. Phys. Chem. A* **2002**, *106*, 6229–6231.
- (34) Borel, A.; Helm, L.; Merbach, A. E. *Chem. Eur. J.* **2001**, *7*, 600–610.
- (35) Bencini, A.; Ciofini, I.; Uytterhoeven, M. G. *Inorg. Chim. Acta* **1998**, *274*, 90–101.